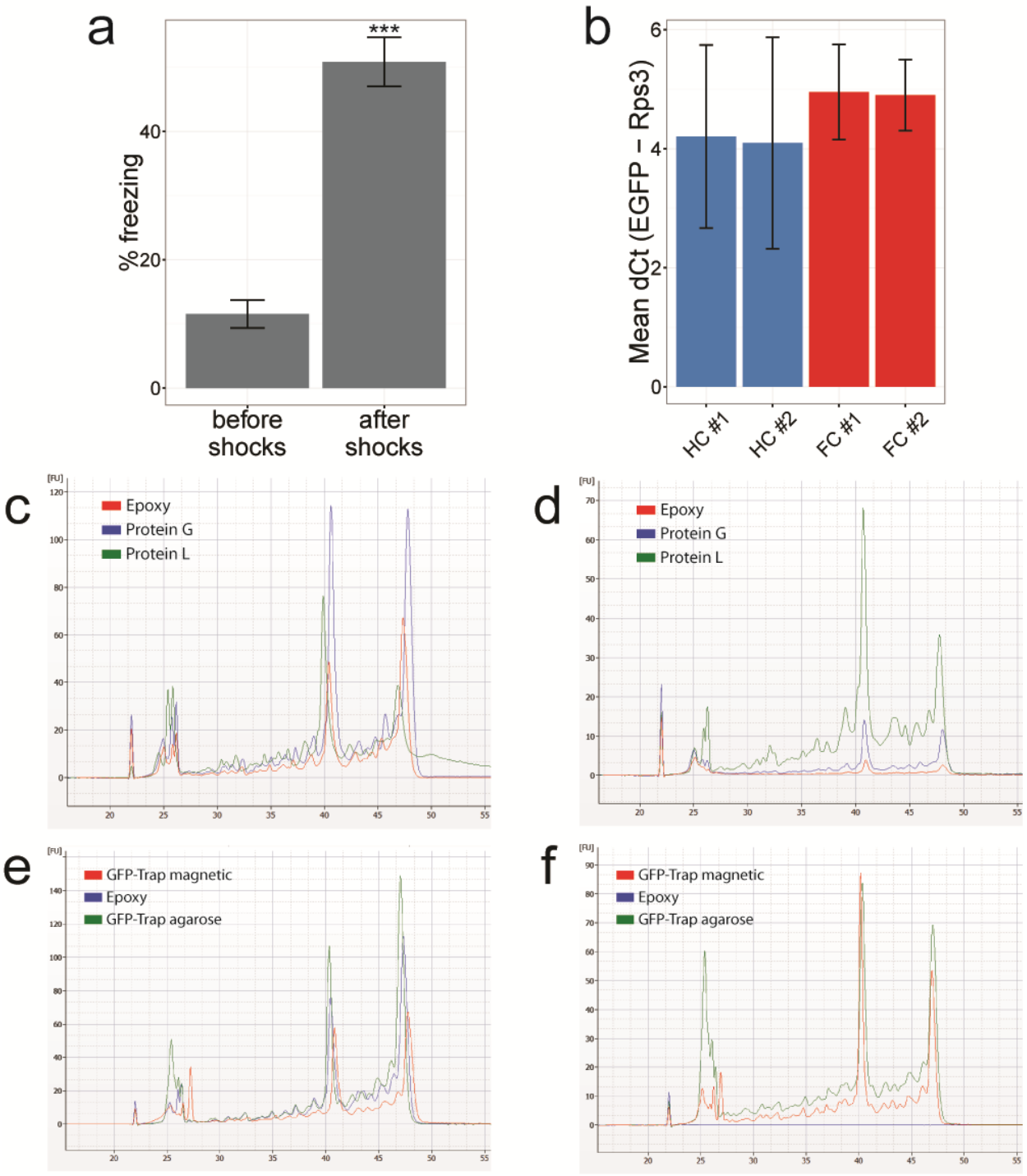

Supplementary Figure 1: Collection of ribosome-bound mRNA from transgenic Camk2a-tTA, tetO-EGFP-L10a mice using an improved protocol for low background ribosome immunoprecipitation. (a) Camk2a-tTA, tetO-EGFP-L10a transgenic mice showed normal fear conditioning. Average percent of time spent freezing for mice before-shocks (minute 2-3 of the protocol) and after-shocks (final 40 seconds of the protocol). (n=8, bars represent SEM, *** = $p < 0.0001$ using paired t-test). (b) Home cage and fear conditioning mice had similar EGFP-L10a

expression. EGFP-L10a expression was measured with qPCR and normalized to Rps3. Mean delta Ct (dCt) was calculated by averaging the dCt for the dendrite IP, dendrite SN, soma IP, and soma SN for each individual mouse. Bars represent SEM. (c-f) Representative Bioanalyzer traces comparing RNA levels for EGFP immunoprecipitation protocols detailed in the Methods. (c&d) Comparison of EGFP immunoprecipitation protocols either using Protein G or Protein L-coated magnetic beads bound to two anti-GFP antibodies or using a glycidyl ether (epoxy) reactive group to covalently link a single anti-GFP antibody to the bead. (c) 10% of a Camk2a-tTA, tetO-EGFP-L10a double transgenic whole brain homogenate was used as input. (d) 10% of a tetO-EGFP-L10a single transgenic whole brain homogenate was used as input as a background control. The epoxy beads resulted in the lowest background level. (e&f) Comparison of GFP-Trap magnetic and agarose beads (ChromoTek) with epoxy beads. (e) 10% of a Camk2a-tTA, tetO-EGFP-L10a double transgenic whole brain homogenate was used as input. (f) 10% of a tetO-EGFP-L10a single transgenic whole brain homogenate was used as input. The epoxy beads again resulted in the lowest background level.

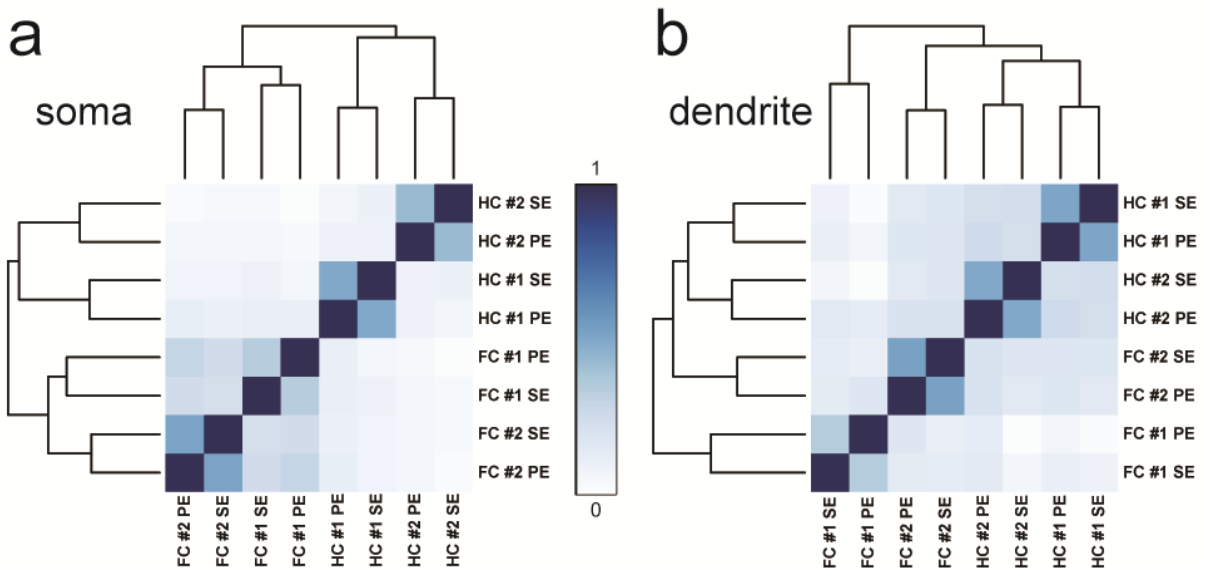

Supplementary Figure 2: Clustering of RNA-Seq IP data. (a,b) Blinded clustering of normalized read counts shows that the immunoprecipitation (IP) samples of the contextual fear conditioned mice cluster apart from the IP samples of the home cage mice, indicating that fear conditioning altered ribosome binding in both the soma (a) and dendrites (b) of CA1 pyramidal neurons. Intensity of blue color represents degree of similarity between samples. Dendrograms on the left and top show the relationship between samples. SE = single end library. PE = paired end library.

a

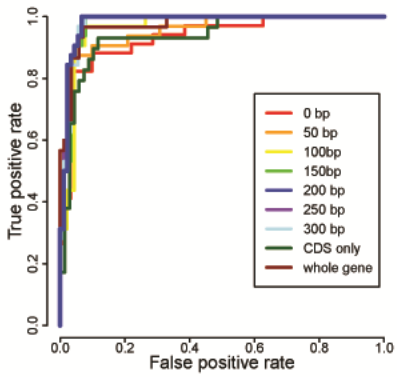

b

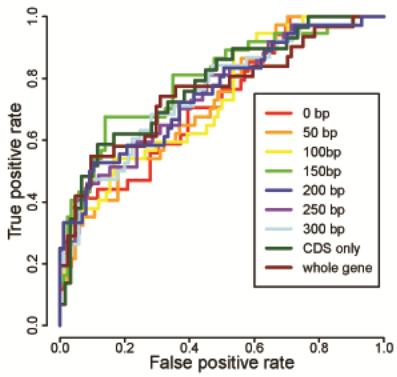

c

Split	Accuracy	Sensitivity	Specificity	AUC	K-1 fold cross validation	Dendritic Genes	Total Genes
000 bp	0.928	0.8235	0.967	0.9343891	90.4	1501	5637
050 bp	0.9431	0.875	0.967	0.9508929	91.05691	1554	5516
100 bp	0.935	0.875	0.956	0.9632555	88.61789	1410	5517
150 bp	0.9421	0.875	0.9663	0.9778792	86.77686	1410	5505
200 bp	0.9344	0.9062	0.9444	0.9819444	90.16393	1890	5478
250 bp	0.9344	0.8438	0.9667	0.9798611	90.16393	1483	5426
300 bp	0.9344	0.8438	0.9667	0.9784722	90.98361	1693	5388
CDS only	0.8247	0.4828	0.9706	0.9366126	81.4433	685	3458
whole gene	0.887	0.6667	0.9647	0.9737255	88.69565	1095	4659

d

Split	Accuracy	Sensitivity	Specificity	AUC	K-1 fold cross validation	Dendritic Genes	Total Genes
000 bp	0.5417	0.8529	0.4186	0.7253762	47.5	4562	5222
050 bp	0.7355	0.24324	0.95238	0.7232947	44.6281	611	5174
100 bp	0.7355	0.5405	0.8214	0.7326255	42.97521	2314	5122
150 bp	0.6423	0.8108	0.5698	0.7960402	56.09756	3913	5059
200 bp	0.6829	0.5833	0.7241	0.7525543	37.39837	2843	5059
250 bp	0.6033	0.8108	0.5119	0.7503218	54.54545	4180	5013
300 bp	0.6016	0.8421	0.4941	0.7563467	57.72358	4229	4983
CDS only	0.7079	0.13793	0.98333	0.7804598	68.53933	204	2856
whole gene	0.7652	0.12903	1	0.7549923	74.78261	117	4097

e

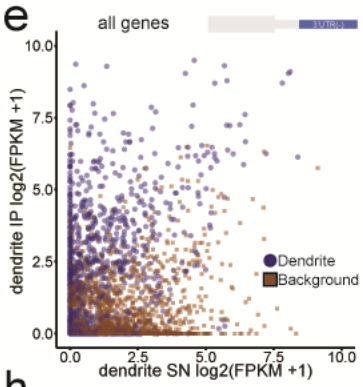

f

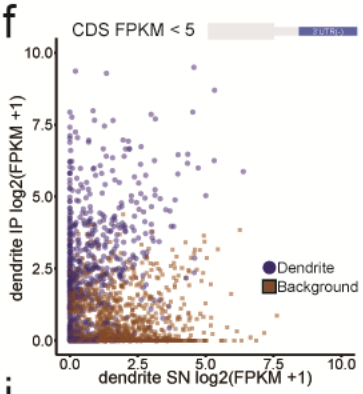

g

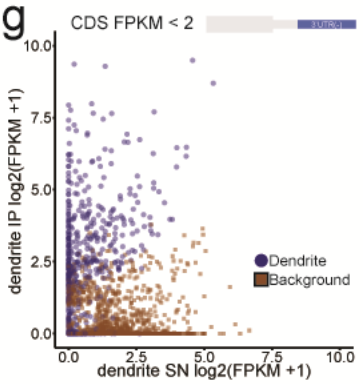

h

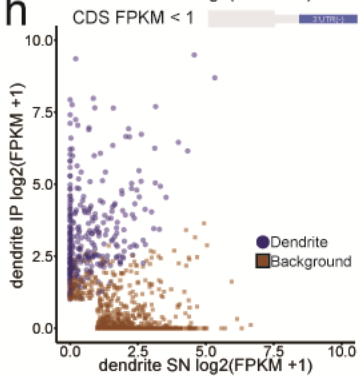

i

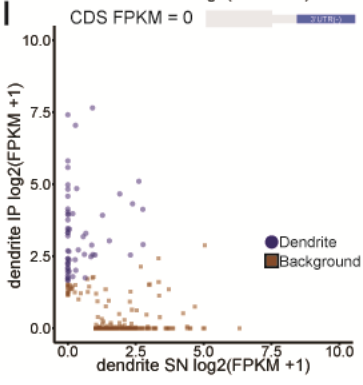

Supplementary Figure 3: Classification results on dendrite data using different 3'UTR splits. (a) Receiver operating characteristic (ROC) curves for contextual fear conditioning dendritic RNA-Seq data with the indicated custom gene models. Whole gene = unaltered UCSC mm9 gene models were used for gene expression quantification with Cufflinks. CDS only = coding sequence models only. 0-300bp = each gene was split into two portions at the indicated distance from the stop codon before expression quantification. (b) ROC curves for home cage dendritic RNA-Seq data with the indicated custom gene models. (c) Table of contextual fear conditioning dendritic RNA-Seq classification results for each gene model. Using the Area Under the ROC Curve (AUC) as a metric combining both sensitivity and specificity, the split at 200bp yields the best results. (d) Table of home cage dendritic RNA-Seq classification results for each gene model. All gene models show poor classification results as predicted by the unclear separation between +pyr and –pyr genes (Fig. 3d). (e) Scatterplot of contextual fear conditioning $FPKM^{3'UTR(-)}$ data showing classification results for all genes. (f) Similar as (e) for genes with $FPKM^{CDS(+)} < 5$. (g) Similar as (e) for genes with $FPKM^{CDS(+)} < 2$. (h) Similar as (e) for genes with $FPKM^{CDS(+)} < 1$. (i) Similar as (e) for genes with $FPKM^{CDS(+)} = 0$. A clear separation between dendritic and background classification becomes apparent when plotting the $FPKM^{3'UTR(-)}$ values for mRNAs with lower $FPKM^{CDS(+)}$ values, illustrating how both the $FPKM^{CDS(+)}$ and $FPKM^{3'UTR(-)}$ values contribute to classification with highest accuracy.

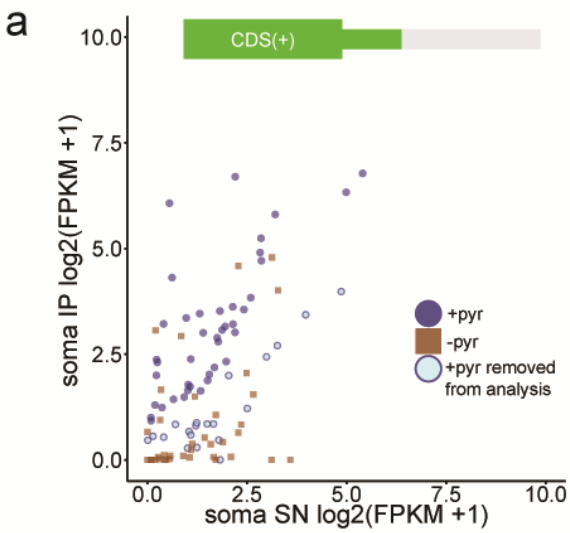

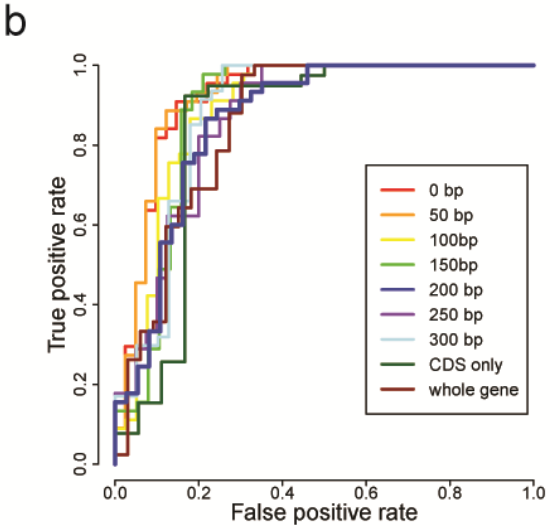

c

Split	Accuracy	Sensitivity	Specificity	AUC	K-1 fold cross validation	Somatic Genes	Total Genes
000 bp	0.7529	0.5909	0.9268	0.9201774	74.11765	1647	5937
050 bp	0.7765	0.6591	0.9024	0.922949	74.11765	1965	5896
100 bp	0.7143	0.5556	0.8974	0.8871795	67.85714	1478	5853
150 bp	0.7229	0.6	0.8684	0.8847953	68.6747	1670	5812
200 bp	0.8293	0.8667	0.7838	0.8624625	73.17073	2903	5778
250 bp	0.7176	0.6444	0.8	0.8661111	70.58824	2411	5755
300 bp	0.7093	0.5745	0.8718	0.8788871	65.11628	1901	5728
CDS only	0.7544	1	0.2222	0.8433048	73.68421	3254	3410
whole gene	0.72	0.619	0.8485	0.8556999	62.66667	1849	4923

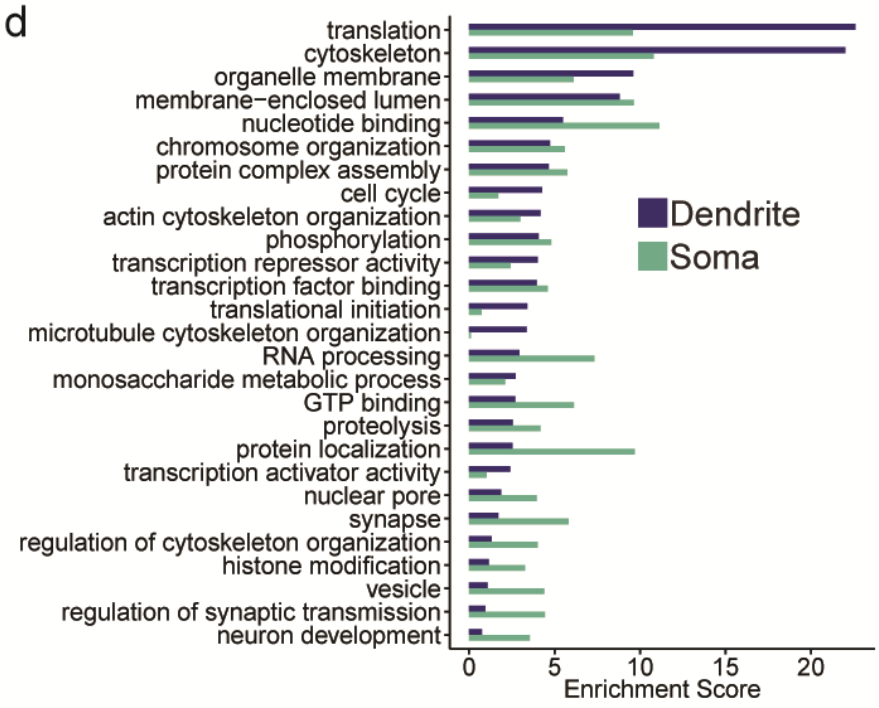

Supplementary Figure 4: Classification results for contextual fear conditioning soma RNA-Seq data using different 3'UTR splits. (a) +pyr and –pyr IP CDS(+) scatterplots for contextual fear conditioning soma. Genes with an IP/SN ratio < 1 were assumed to be present in pyramidal neurons but not bound to ribosomes at sufficient levels for IP enrichment and were excluded as training genes in the classification for the somatic data. (b) ROC curves for contextual fear conditioning somatic RNA-Seq data with the indicated custom gene models as detailed in Supplementary Fig. 3. The line for the 200bp split is highlighted. (c) Table of classification results for each gene model. While the 200bp CDS(+)/3'UTR(-) split gene model does not have the highest area under the ROC curve (AUC), it does have the best balance between sensitivity and specificity and was used for final classification results. (d) Top 20 enriched GO categories for dendritic and somatic mRNAs organized by level of dendritic enrichment.

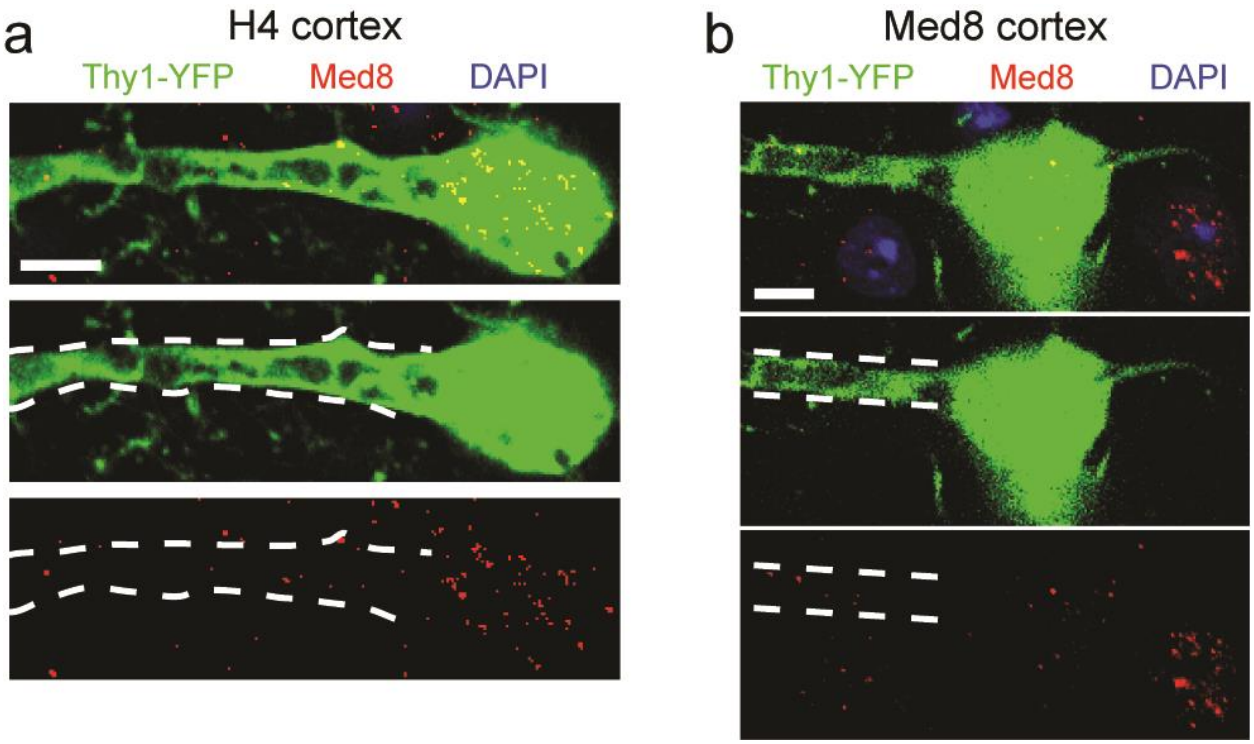

Supplementary Figure 5: Detection of Histone H4 and Med8 proteins within dendrites of cortical pyramidal neurons. (a) Immunohistochemical labeling of Histone H4 in a Thy1-YFP labeled cortical neuron. red = Histone H4, green = Thy1-YFP. The dashed white lines outline the dendrite. (b) Immunohistochemical labeling of Med8 in Thy1-YFP labeled cortical neuron. red = Med8, green = Thy1-YFP, blue = DAPI. The dashed white lines outline the dendrite. Scale Bars = 10μm.

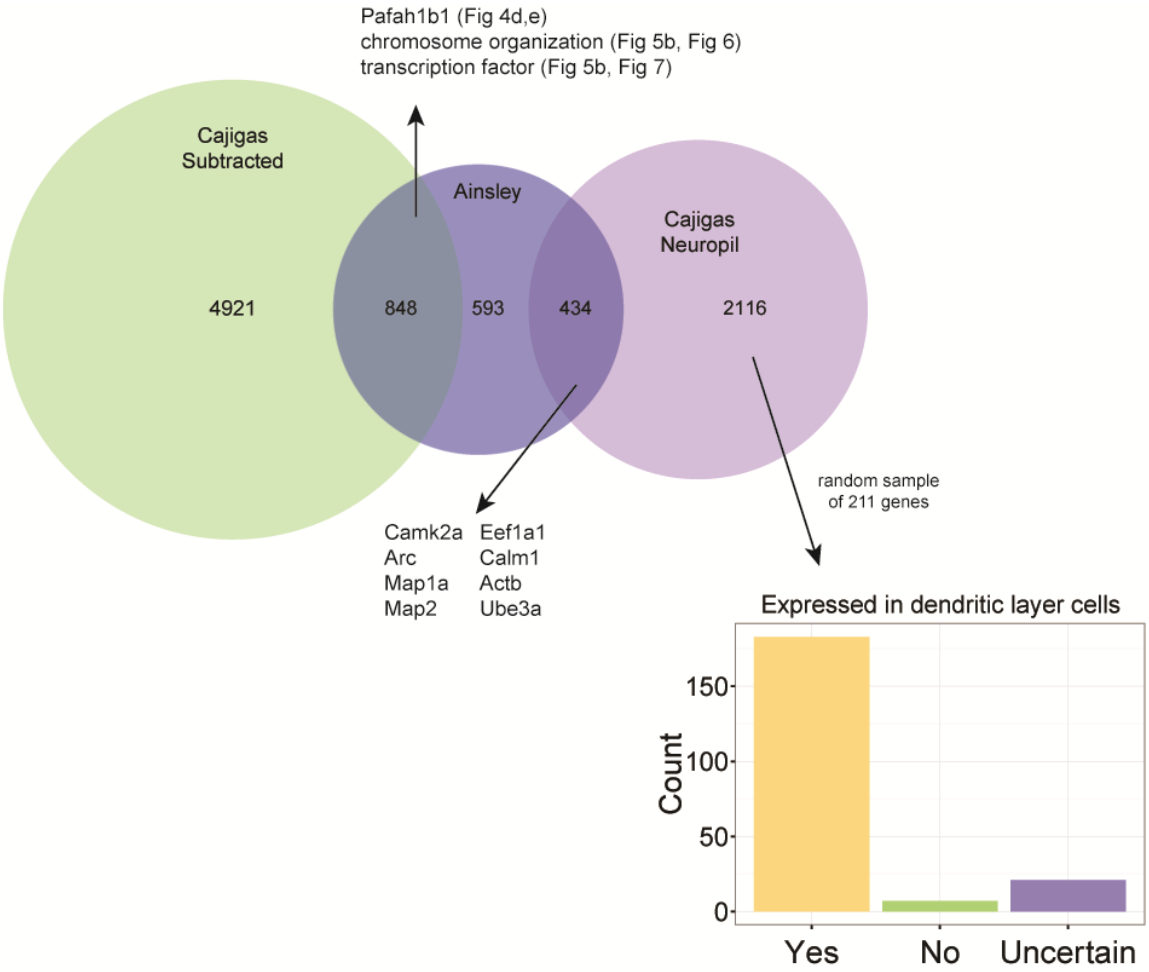

Supplementary Figure 6. Comparison between dendritic gene lists from current study and Cajigas, et. al. The Venn diagram shows the overlap between the current study (Ainsley), the filtered list of neuropil genes identified by Cajigas, et. al. [1] (Cajigas Neuropil), and the list of genes subtracted from the neuropil gene list (Cajigas Subtracted) in Cajigas, et. al. for reasons including expression in non-pyramidal neuron cell types or association with nuclear functions. The 434 genes identified by both studies include common dendritic transcripts (8 examples listed). The 848 genes that are in both Ainsley and Cajigas Subtracted could represent false negatives in Cajigas, et. al., as confirmed for 3 genes that fall within subtracted categories (Fig. 4d,e, Fig. 6, Fig. 7). A random sample of 10% of the 2116 genes detected by Cajigas, et. al., but not by our study, were screened using Allen Mouse Brain Atlas *in situs* for expression within cells in the dendritic layer (i.e. cells located in the stratum lacunosum moleculare or stratum radiatum of the CA1 region of the hippocampus). A gene was labeled as Yes if expression could be seen in dendritic layer cells, No if expression was limited to the stratum pyramidale (location of pyramidal cell bodies), and Uncertain if the *in situ* experiment was inconclusive or did not exist (see Supplementary Data 4). These data are summarized in the bar chart. Cajigas, et. al. employed microdissection of the dendritic layer followed by RNA-Seq of all collected mRNA transcripts. This method does not allow the prediction of dendritic localization of mRNAs that are also present in dendritic layer cells. While extensive filtering was used to remove mRNAs that could have originated from dendritic layer cells, *in situ* experiments from the Allen Mouse

Brain Atlas show that the vast majority of the Cajigas Neuropil genes not identified in our study show expression in dendritic layer cells and represent potential false positives in Cajigas, et. al. (87% including all randomly sampled genes, 96% excluding genes labeled Uncertain).

Mouse	Behavior	Location	Sample	Sequencing Type	Total Reads	STAR Alignments	STAR Uniques
HC#1	home cage	dendrite	immunoprecipitate	single end	8177076	2448748	1445297
HC#1	home cage	soma	immunoprecipitate	single end	8857590	2569133	1638686
HC#1	home cage	dendrite	immunoprecipitate	paired end	64774840	22663322	13839586
HC#1	home cage	soma	immunoprecipitate	paired end	131280050	42852341	30592880
HC#2	home cage	dendrite	immunoprecipitate	single end	2217975	564322	298102
HC#2	home cage	dendrite	supernatant	single end	12639045	11777311	7344906
HC#2	home cage	soma	immunoprecipitate	single end	8546990	4763727	2058849
HC#2	home cage	dendrite	immunoprecipitate	paired end	214610116	66945555	42993182
HC#2	home cage	dendrite	supernatant	paired end	93163380	87606290	74757988
HC#2	home cage	soma	immunoprecipitate	paired end	73420060	41391241	32773341
FC#1	fear conditioned	dendrite	immunoprecipitate	single end	9107338	3614656	2402299
FC#1	fear conditioned	soma	immunoprecipitate	single end	8285494	4566140	3667054
FC#1	fear conditioned	dendrite	immunoprecipitate	paired end	108448502	86803138	57233931
FC#1	fear conditioned	soma	immunoprecipitate	paired end	77679718	51637767	43115178
FC#2	fear conditioned	dendrite	immunoprecipitate	single end	8874255	3025743	1788058
FC#2	fear conditioned	dendrite	supernatant	single end	8632308	7966387	4587254
FC#2	fear conditioned	soma	immunoprecipitate	single end	9308237	4525411	2729574
FC#2	fear conditioned	soma	supernatant	single end	8134420	7646754	3891759
FC#2	fear conditioned	dendrite	immunoprecipitate	paired end	149105624	74577311	46498876
FC#2	fear conditioned	dendrite	supernatant	paired end	87811136	87791965	75868211
FC#2	fear conditioned	soma	immunoprecipitate	paired end	134445102	82517092	64079881
FC#2	fear conditioned	soma	supernatant	paired end	64056566	62358423	52178497

Supplementary Table 1: Summary table of all mice used for RNA-Seq experiments.

Supplementary Reference

1. Cajigas, I. J. *et al.* The Local Transcriptome in the Synaptic Neuropil Revealed by Deep Sequencing and High-Resolution Imaging. *Neuron* **74,** 453–466 (2012).